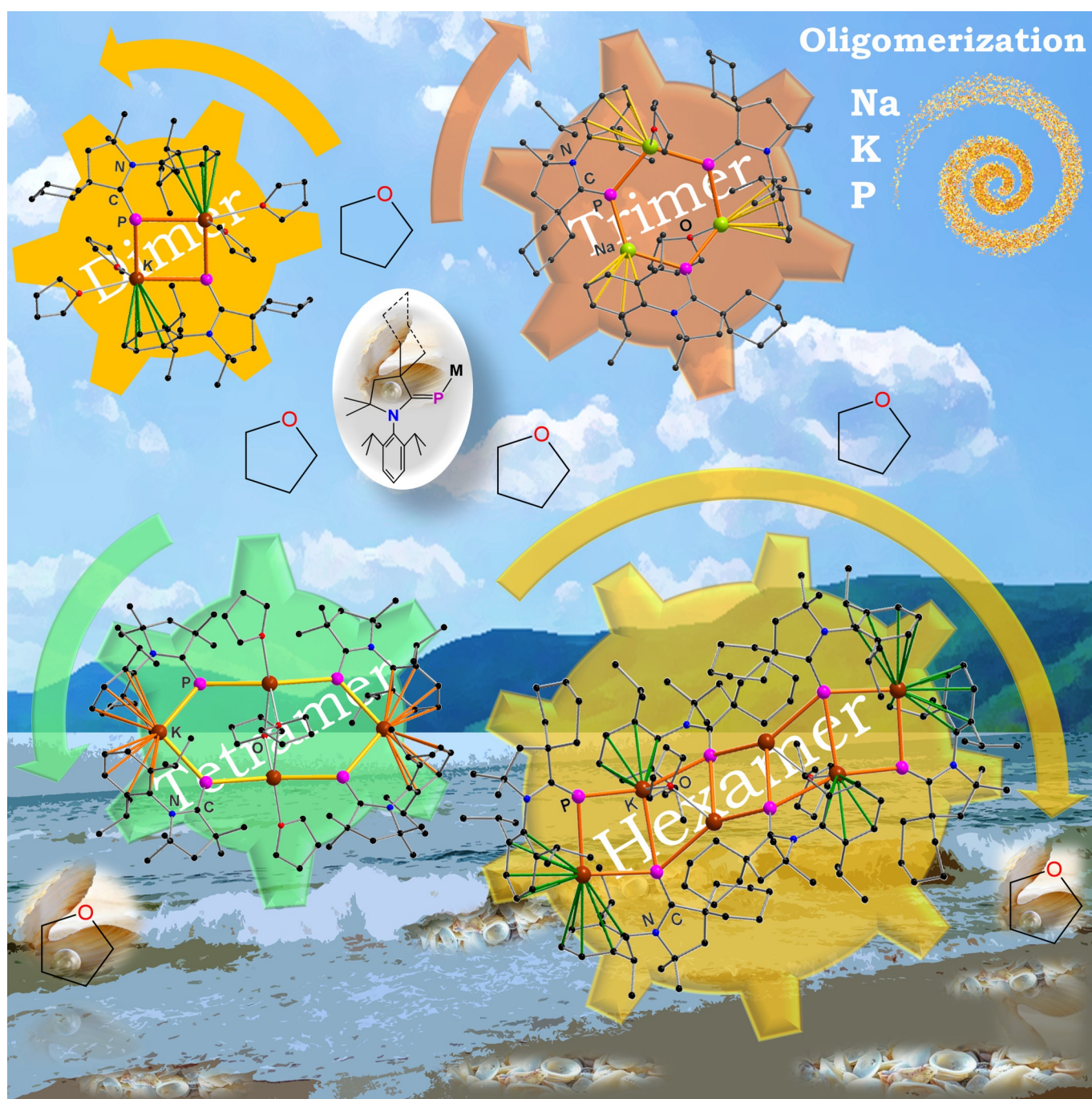


■ Oligomerization

Solid-State Isolation of Cyclic Alkyl(Amino) Carbene (cAAC)-Supported Structurally Diverse Alkali Metal-PhosphinidenidesAditya Kulkarni,^[a] Selvakumar Arumugam,^[b] Maria Francis,^[a] Pulikanti Guruprasad Reddy,^[a] Ekta Nag,^[a] Sai Manoj N. V. T. Gorantla,^[b] Kartik Chandra Mondal,^{*[b]} and Sudipta Roy^{*[a]}

Abstract: Cyclic alkyl(amino) carbene (cAAC)-supported, structurally diverse alkali metal-phosphinidenides **2–5** of general formula $((\text{cAAC})\text{P-M})_n(\text{THF})_x$ [**2**: M=K, $n=2$, $x=4$; **3**: M=K, $n=6$, $x=2$; **4**: M=K, $n=4$, $x=4$; **5**: M=Na, $n=3$, $x=1$] have been synthesized by the reduction of cAAC-stabilized chloro-phosphinidene $\text{cAAC}=\text{P-Cl}$ (**1**) utilizing metallic K or KC_8 and Na-naphthalenide as reducing agents. Complexes **2–5** have been structurally characterized in solid state by NMR studies and single crystal X-ray diffraction. The proposed mechanism for the electron transfer process has been well-supported by cyclic voltammetry (CV) studies and Density Functional Theory (DFT) calculations. The solid state oligomerization process has been observed to be largely dependent on the ionic radii of alkali metal ions, steric bulk of cAAC ligands and solvation/de-solvation/recombination of the dimeric unit $[(\text{cAAC})\text{P-M}(\text{THF})_x]_2$.

The reactive group 15 analogs of carbenes, known as phosphinidenes have been initially identified in gas phase and by low temperature matrix isolation.^[1] The stable, structurally characterizable phosphinidenes have been synthesized either in presence of transition metals^[2] or as carbene-phosphinidene adducts, known as parent phosphinidenes.^[3–5] Metal-phosphinidenes (or phosphinidenyls) are the reactive analogues of metal phosphides^[6] with low valent, low coordinate phosphorus atoms. Such species could be synthetically achieved by strong base mediated deprotonation of the parent phosphinidenes^[3–5] as the corresponding conjugate bases.^[7] A decade ago, *N*-heterocyclic carbene (NHC)-supported phosphinidene $[(\text{THF})_3\text{Li-L}=\text{P-H}]$ had been synthesized by direct reduction of $\text{L}=\text{P}=\text{P}=\text{L}$ ($\text{L}=\text{NHC}$).^[3a] The modified, neutral $\text{L}=\text{P-H}$ has been synthesized by the oxidation of $\text{L(H)}(\text{PH}_2)$ by activating the P-H_{PH_2} bond. Another variant of $\text{L}=\text{P-H}$ has been prepared by reacting the corresponding imidazolium salt with Na_3P_7 in THF ($\text{L}=\text{saturated NHC}$).^[3c] A few other synthetic routes for phosphinidenes have also been reported.^[3] Recently, Roesky et al. developed a synthetic route for cyclic (alkyl)amino carbene (cAAC)-supported chloro-phosphinidenes $\text{cAAC}=\text{P-Cl}$ (**1**), where two equiv of free cAAC reacted with one equiv of PCl_3 at room temperature under reductive elimination of $\text{cAAC-Cl}^+\text{Cl}^-$ salt.^[4b] Later on, the chlorine atom of **1** was substituted by the hydride donor LiAlH_4 in toluene to obtain $\text{cAAC}=\text{P-H}$. However,

this reaction was not thermodynamically well controlled, leading to the co-crystallization of $\text{cAAC}=\text{P-Cl}/\text{cAAC}=\text{P-H}$. $\text{cAAC}=\text{P-H}$ was characterized only in solution by NMR studies.^[4b] Deprotonation of $\text{cAAC}=\text{P-H}$ by Me-Li in THF led to the formation of the dimeric, THF-coordinated lithium-phosphinidenide $[(\text{Me}_2\text{-cAAC})\text{P-Li}(\text{THF})_2]_2$, which was shown to react with various halogen containing inorganic and organic compounds in solution.^[8] The monomeric potassium-phosphinidenide $[(\text{Me}_2\text{-cAAC}/\text{NHC})\text{P-K}]$ was in situ generated by reacting $\text{cAAC}=\text{P-H}$ with the potassium salt of benzyl-anion ($\text{Ph-CH}_2\text{-K}$) and further reacted without solid state structural characterization of $(\text{Me}_2\text{-cAAC}/\text{NHC})\text{P-K}$ (Scheme 1).^[9–10]

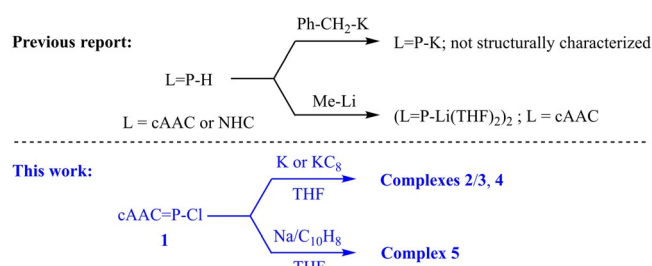
Several other main group- or metal-phosphinidenes and mixed NHC-based-phosphinidenes/alkoxides have also been reported.^[9–11] Herein, we report the first alkali metal mediated direct reduction of carbene-supported chloro-phosphinidenes $\text{cAAC}=\text{P-Cl}$ (**1**) for the syntheses and solid state characterization of various oligomeric metal-phosphinidenides **2/3–5** $((\text{cAAC})\text{P-M})_n(\text{THF})_x$ [**2**: M=K, $n=2$, $x=4$; **3**: M=K, $n=6$, $x=2$; **4**: M=K, $n=4$, $x=4$; **5**: M=Na, $n=3$, $x=1$].

Cyclic voltammetry (CV) studies of cyclic alkyl(amino) carbene (cAAC)-stabilized chloro-phosphinidene $\text{Cy-cAAC}=\text{P-Cl}$ [$\text{Cy-cAAC}=\text{:C}(\text{N-2,6-}i\text{Pr}_2\text{C}_6\text{H}_3)(\text{C}_6\text{H}_{10})(\text{CMe}_2)(\text{CH}_2)$] (**1a**)^[4] in 0.1 M solution of $[\text{nBu}_4\text{N}]\text{PF}_6$ in THF showed a possible one electron quasi-reversible reduction at $E_{1/2} = -2.85$ V indicating the generation of the corresponding radical intermediate $(\text{Cy-cAAC})\text{P}^{\cdot-}$ (**Int-1a**) (Figure 1, left). Triggered by this result, we envisioned a possible reduction of **1**. Accordingly, a reaction was set up using KC_8 as the initial reducing agent. The 1:3 molar mixture of fluorescent yellow $\text{Cy-cAAC}=\text{P-Cl}$ (**1a**) and KC_8 were placed in a Schlenk flask, kept in ice/water bath ($0-4^\circ\text{C}$) under argon atmosphere. Precooled ($0-4^\circ\text{C}$) THF was added to the solid mixture via a cannula. The temperature of the reaction mixture was slowly raised to room temperature, while the color changed from yellow to bright orange after 15 min and further changed to dark green after another 15–20 min. The reaction mixture was stirred for 12 h at room temperature to obtain a dark red color, which was then filtered to separate out the graphite. Gratifyingly, dark red crystals (rod/hexagonal) of complexes **2a/3** $[(\text{cAAC})\text{P-M})_n(\text{THF})_x$; M=K, $n=2$, $x=4$ (**2a**); M=K, $n=6$, $x=2$ (**3**)] were obtained after one day from the concentrated THF solution kept in a refrigerator at 0°C (Scheme 2). Under similar reaction conditions, $\text{Me}_2\text{-cAAC}=\text{P-Cl}$ (**1b**) [$\text{Me}_2\text{-cAAC}=\text{:C}(\text{N-2,6-}i\text{Pr}_2\text{C}_6\text{H}_3)(\text{CMe}_2)(\text{CH}_2)$] produced dark red crystals of tetrameric complex **4** $[(\text{cAAC})\text{P-M})_4(\text{THF})_4$] (Scheme 3,

[a] A. Kulkarni, M. Francis, P. G. Reddy, E. Nag, Dr. S. Roy
Department of Chemistry
Indian Institute of Science Education and Research (IISER)
Tirupati 517507 (India)
E-mail: roy.sudipta@iisertirupati.ac.in

[b] S. Arumugam, S. M. N. V. T. Gorantla, Dr. K. C. Mondal
Department of Chemistry
Indian Institute of Technology Madras
Chennai 600036 (India)
E-mail: csdkartik@iitm.ac.in

 Supporting information and the ORCID identification number(s) for the author(s) of this article can be found under:
 <https://doi.org/10.1002/chem.202003505>.



Scheme 1. Synthetic routes for metal-phosphinidenides.

left). The use of K metal as the reducing agent also led to the formation of complexes **2–4** under similar reaction conditions in comparable yields.

The trimeric sodium-phosphinidenide $((\text{Cy-cAAC})\text{P-Na})_3(\text{THF})$ (**5**) was obtained upon treating compound **1a** with freshly-prepared Na-naphthalenide ($\text{Na}/\text{C}_{10}\text{H}_8$) in 1:2.2 molar ratio in THF at room temperature for 12 h. Hexagonal, orange-red crystals of **5** were obtained from a concentrated THF solution at 0°C (Scheme 3, right). However, the use of Na metal as reducing agent failed to afford complex **5** under similar reaction condition.

Single crystal X-ray diffraction revealed that complexes **2a–5** are THF-solvated dimeric (**2a**), hexameric (**3**), tetrameric (**4**) and trimeric (**5**) forms of the monomeric unit $\text{cAAC}=\text{P-M}$ (Schemes 2–4, Figures 3–5). The crystals and concentrated THF solutions of **2a–5** were found to be stable under argon atmosphere for several months at room temperature. However, the red powders of **2a–5** were observed to change color immediately from red to yellow upon exposure to air due to the formation of $\text{cAAC}=\text{P-H}$ (**6**) as confirmed by ^{31}P NMR spectroscopy (Figure S20).^[4b] The isolated yields of complexes **2a–5** were found to be in the range of 65–67%. A small amount of $\text{cAAC}=\text{P-H}$ (**6a** ($\text{Cy-cAAC}=\text{P-H}$); **6b** ($\text{Me}_2\text{-cAAC}=\text{P-H}$))^[4b] and $(\text{cAAC})_2\text{P}_2$ (**Int-2a** ($((\text{Cy-cAAC})_2\text{P}_2)$); **Int-2b** ($((\text{Me}_2\text{-cAAC})_2\text{P}_2)$); Scheme 4) were also isolated during the reaction, which were separated by filtration of the crystals of complexes **2a–4**. The by-products **6a** and **Int-2a**^[12] were further characterized by NMR spectroscopy and X-ray single-crystal diffraction (see Supporting Information).

Upon dissolving the complexes **2a/3** in THF containing around 70 ppm of water led to the formation of protonated by-product **6a**. The calculated proton affinity value of $\text{Me}_2\text{-cAAC}=\text{P}^-$ anion ($+371\text{ kcal mol}^{-1}$) was found to be 54 kcal mol^{-1} lower than that of $n\text{Bu-Li}$ (425 kcal mol^{-1}) as expected (see Supporting Information).

To have a deeper insight into the reaction mechanism, a set of reactions have been carried out followed by CV studies of the reaction solutions (Figure 1).

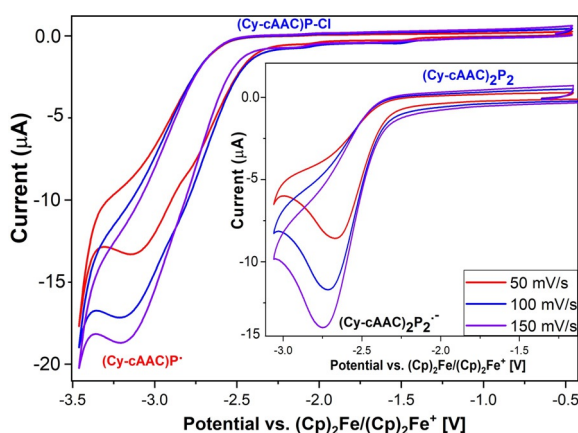
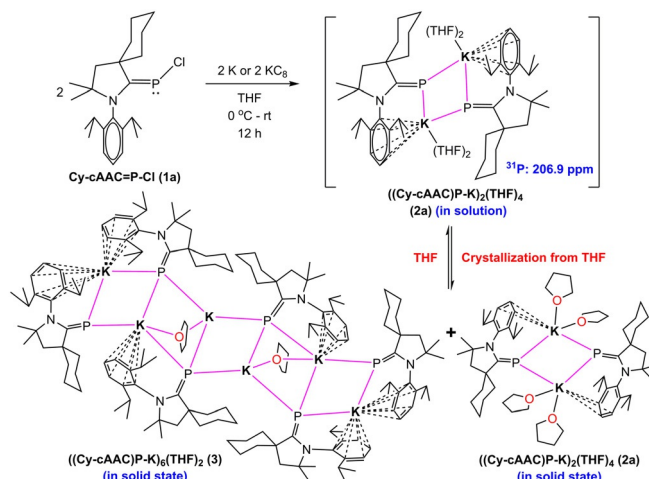
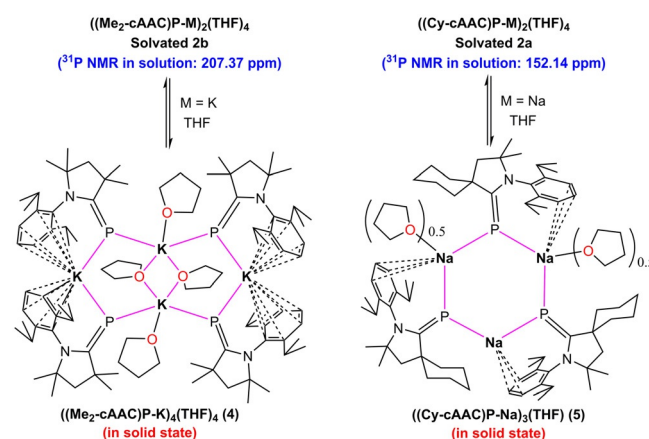


Figure 1. Cyclic voltammograms of $\text{Cy-cAAC}=\text{P-Cl}$ (**1a**) (left) and $(\text{Cy-cAAC})_2\text{P}_2$ (**Int-2a**) (inset) in THF containing $0.1\text{ M } [n\text{Bu}_4\text{N}]\text{PF}_6$ as the electrolyte (CE: Pt, WE: GC, RE: Ag).

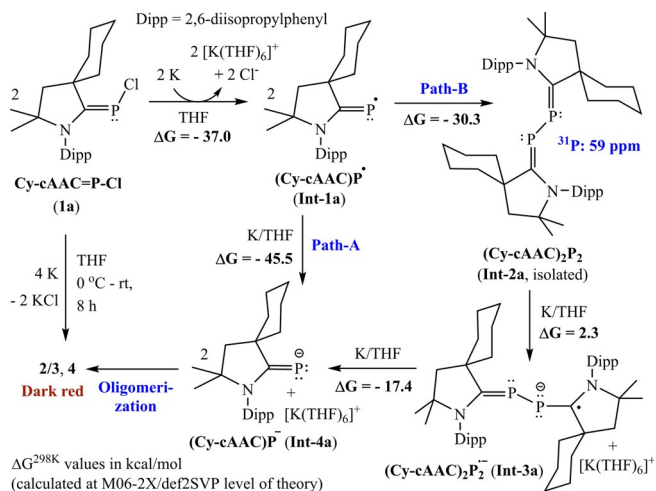


Scheme 2. Synthesis of cAAC -supported dimeric $[((\text{Cy-cAAC})\text{P-K})_2(\text{THF})_4]$ (**2a**) and hexameric $[((\text{Cy-cAAC})\text{P-K})_6(\text{THF})_2]$ (**3**) potassium-phosphinidenides.



Scheme 3. Syntheses of tetrameric $[((\text{Me}_2\text{-cAAC})\text{P-K})_4(\text{THF})_4]$ (**4**) potassium- and trimeric $[((\text{Cy-cAAC})\text{P-Na})_3(\text{THF})]$ (**5**) sodium-phosphinidenides.

One equiv of K-metal was reacted with $\text{Cy-cAAC}=\text{P-Cl}$ (**1a**) to produce $(\text{Cy-cAAC})_2\text{P}_2$ (**Int-2a**) which was confirmed by NMR studies. This indicated that the first electron transfer from K to **1a** occurred to form the intermediate radical species $(\text{Cy-cAAC})\text{P}^\cdot$ (**Int-1a**) and KCl. The color of the solution at the surface of the solid K-metal appeared as dark red, while the color of the bulk solution was always observed to be yellow $[\text{K} + \text{Cy-cAAC}=\text{P-Cl} = (\text{Cy-cAAC})\text{P}^\cdot + \text{KCl}; (\text{Cy-cAAC})\text{P}^\cdot + \text{K} = (\text{Cy-cAAC})\text{P-K}; (\text{Cy-cAAC})\text{P-K} + \text{Cy-cAAC}=\text{P-Cl} = (\text{Cy-cAAC})_2\text{P}_2 + \text{KCl}]$. It was observed that two equiv of K-metal ($E_{1/2} = -2.93\text{ V}$) can also quantitatively reduce **1a** to dark red complexes **2a/3** in THF after 12 h. This was further confirmed by NMR spectroscopy. In contrast, Na-metal ($E_{1/2} = -2.71\text{ V}$) was unable to reduce **1a**; both the starting materials remained unreacted even after 2 days. The cyclic voltammogram of **1a** shows the first e^- transfer [$E_{1/2} < -2.85\text{ V}$] corresponding to the one electron quasi-reversible process ($\Delta V_{\text{peak-peak}} = 0.71\text{ V}$) at scan rate of 50 mV s^{-1} (i.e. from K-metal to the **1a**) suggesting the generation of **Int-1a** (Figure 1). The irreversible process [$E_{1/2} <$



Scheme 4. Mechanism for the generation of cAAC-supported potassium-phosphinidenides **2a/3-4** in THF (see Supporting Information for Me₂-cAAC analogs).

–2.55 V; Figure 1 (inset)] corresponding to the successive e[–] transfer occurred spontaneously from K-metal to the stable intermediate ((Cy-cAAC)₂P)₂ (**Int-2a**) leading to the formation of ((Cy-cAAC)₂P)₂^{•–}/((Cy-cAAC)P)^{•–}. Similarly, Na/C₁₀H₈ could act like K-metal in solution to produce the trimeric complex **5**. The computed ΔG^{298K} for the electron transfer from SUMO_{Nap}^{•–} to LUMO_{Cy-cAAC=P-Cl} is –11.5 kcal mol^{–1}.

A plausible mechanism for the reduction of **1a** was proposed based on CV and NMR studies which were further supported by theoretical calculations (Scheme 4).

Theoretical calculations showed that the proposed (indicated by CV) conversion of Cy-cAAC=P-Cl (**1a**) to cAAC=P[•] radical (**Int-1a**) is exothermic by –18.5 kcal mol^{–1}. Once the high energy radical intermediate **Int-1a** is formed, it can follow two competing pathways: Path-A and Path-B (Scheme 4). In Path-A, the electron transfer from K to **Int-1a** (–22.8 kcal mol^{–1}) is believed to be crucial. Whereas, Path-B is the highly probable dimerization of **Int-1a** to produce the stable intermediate **Int-2a** ((Cy-cAAC)₂P)₂ which was also found to be exothermic (–30.3 kcal mol^{–1}) and slightly more favorable when compared to path-A. This was evident from the fact that, we could experimentally isolate **Int-2a** in higher yield, when the reaction time was reduced to less than 4 h. A similar reaction in C₆D₆ showed the formation of solvent free, dimeric ((Cy-cAAC)P-K)₂ and ((Cy-cAAC)₂P)₂, evident from the ³¹P resonances at 186.3 and 55.9 ppm, respectively after 24 h, where the later was found to be the major product (Figure 2).

A previously reported silicon analogue ((cAAC)₂Si₂) of ((Cy-cAAC)₂P)₂ (**Int-2a**) is known to accept an electron to form the corresponding radical anion ((cAAC)₂Si₂)^{•–}.^[13] The conversion of **1a** to **Int-2a** was theoretically found to be overall exothermic. Geometry optimization followed by frequency calculations (at M06-2X/def2SVP level of theory) of **Int-2a** suggested the favorable one electron reduction of **Int-2a** leading to the formation of the mono-radical anion ((cAAC)₂P)₂^{•–} (**Int-3a**, +2.2 kcal mol^{–1}) which can further dissociate to produce the monomeric intermediate **Int-4** (–17.4 kcal mol^{–1}).

Complexes **2a/3-5** have been characterized by ¹H, ¹³C and ³¹P NMR spectroscopic analysis. In all the cases the NMR spectra recorded for in situ generated complexes in THF-D₈ and isolated pure crystalline complexes have been found to be identical. The temperature dependent ¹H NMR spectra of complexes **2a-4** in THF-D₈ remains unchanged from room temperature down to –90 °C (see Supporting Information). The ³¹P NMR spectra of complexes **2a-5** show broad singlets with two satellites (due to P–C coupling) in the range of 200–210 ppm for **2a/3, 4** (see Supporting Information) which is highly downfield shifted when compared to the reported dimeric species [cAACPLi(THF)₂]₂ (+177.34 ppm)^[8] indicating more double bond character of the P–C_{cAAC} bond (C–P 1.7036(12), C–N 1.3955(14) Å). The ³¹P NMR spectrum of complex **5** shows a broad singlet at 152 ppm. The ¹³C NMR spectra of complexes **2a-5** show doublets (*J*_{C-P} = 80–82 Hz for **2a/3, 4**; *J*_{C-P} = 104 Hz for **5**) corresponding to C_{cAAC} in the range of 202–208 ppm. The solution NMR studies of complexes **2a-5** suggest that all these complexes are either monomeric or dimeric [(cAAC-P)₂K₂(THF)_x]. The comparatively downfield chemical shift values of complexes **2a/3** can be attributed to the stronger π-back donation from P to C_{cAAC} in complexes **2a/3** (C–P 1.6764(1), C–N 1.4129(1) Å). The computed ³¹P chemical shift value for complex **2a** is 210.3 ppm which is very close to that of the experimental value. The ¹³C NMR studies in solid state (Figures S7, S13) and solution (Figures S8, S14) clearly suggest that the structures of complexes **2a-4** in solid state are profoundly different when compared to that in their respective solutions. At –70 °C, the coupling constant, *J*_{C-P} was found to be 72.1 Hz for complexes **2a/3**, whereas the same for complex **4** was found to be 28.3 Hz in THF-D₈.

The X-ray single-crystal diffraction revealed that complex [(Cy-cAAC-P)₂K₂(THF)₄] (**2a**) (for molecular structure see Supporting Information) co-crystallizes with complex [(Cy-cAAC-P)₆K₆(μ-THF)₂] (**3**) in triclinic *P*-1 space group as [(Cy-cAAC-P)₆K₆(THF)₂][(Cy-cAAC-P)₂K₂(THF)₄]₂·2THF. The molecular structure of complex **3** is depicted in Figure 3 for connectivity of the atoms (see Supporting Information for details).

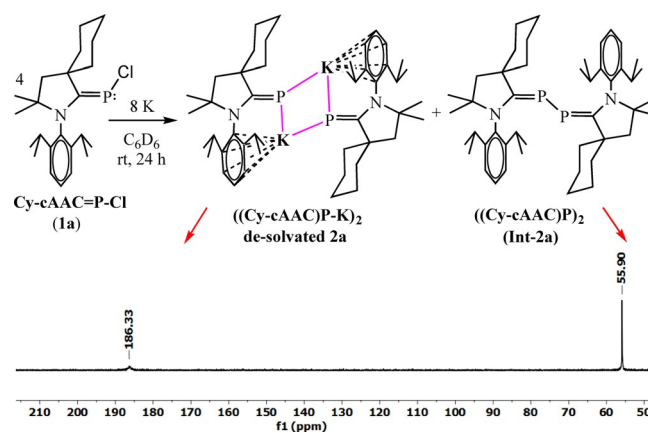


Figure 2. Formation of ((Cy-cAAC)P-K)₂ (de-solvated **2a**; ³¹P: 186.33 ppm) and ((Cy-cAAC)₂P)₂ (**Int-2a**; ³¹P: 55.90 ppm) after 24 h in C₆D₆.

Complex **4** $[(\text{Me}_2\text{-cAAC-P})_4\text{K}_4(\mu\text{-THF})_2(\text{THF})_2]$ crystallizes as **4-2(THF)** in monoclinic $P2_1/c$ space group and the molecular structure is shown in Figure 4.

The asymmetric unit of the tetrameric complex **4-2(THF)** consists of two $\text{Me}_2\text{-cAAC}=\text{P}^-$ anions, two K^+ ions and two THF molecules. Additionally, a lattice THF molecule also crystallizes in the asymmetric unit. Complex **4** possesses a centre of symmetry and two mirror planes passing through K1 to bisect the molecule into two equal halves (see Supporting Information). The P atoms in each $\text{Me}_2\text{-cAAC}=\text{P}^-$ anionic unit show trigonal planar geometry (the sum of the bond angles is close to 360°) by coordinating with the adjacent K1 and K4 atoms. In other words, two of each $\text{Me}_2\text{-cAAC}=\text{P}^-$ units are shared by two adjacent K^+ ions in such a way that the overall charge is balanced in the structure. On the other hand, K4 also strengthens the structure by coordinating with a terminal and a bridging THF molecules as well as with two adjacent $\text{Me}_2\text{-cAAC}=\text{P}^-$ anionic units. The K_4P_4 butterfly like core is non-planar having two K^+ ions at the body position, bridged by two $\mu\text{-THF}$ adopting a distorted trigonal pyramidal coordination geometry. These two K^+ ions have adopted distorted square pyramidal geometry. Other two K^+ ions at the wing positions are being sandwiched by two aromatic rings in bent fashion. The average P-K distances in **4** are lying in the range of 3.2761(10)–3.3532(10) Å which are close to those of **3** and tetrameric $[(2,6\text{-dimesitylphenyl})\text{P}(\text{H})\text{K}]_4$ complex.^[6c] The average K-P-K/P-K-P bond angles in **4** are found in the range of 123.87–125.23°/97.49–157.07°. Complex **5** $[(\text{Cy-cAAC-P})_3\text{Na}_3(\text{THF})]$ crystallizes as **5-2(THF)** in monoclinic $C2/c$ space group. The molecular structure is depicted in Figure 5.

The asymmetric unit of the trimeric complex **5** consists of three Na^+ ions and three $\text{Cy-cAAC}=\text{P}^-$ moieties. Three μ -bridging P-atoms of three $\text{Cy-cAAC}=\text{P}^-$ anions connect the three Na^+ ions in a cyclic fashion to form a trimer containing a non-planar Na_3P_3 unit (Figure S30). One of the three Na^+ ions is terminally coordinated by one THF molecule. There are two half-occupied disordered-THF molecules coordinated to Na^+ ions ($\text{Na1}/\text{Na3}$) filling the void space between the two trimers (evident from the space filling packing diagram).^[14] The third Na^+ ion (Na2) is not coordinated by any THF molecule. All three Na^+ ions are interacting with the phenyl ring of Dipp-group

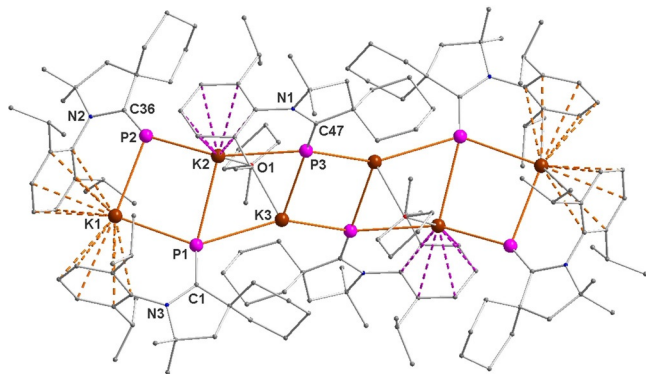


Figure 3. Molecular structure of complex **3** (depicted for atom connectivity only). H atoms and lattice THF molecules were omitted for clarity.

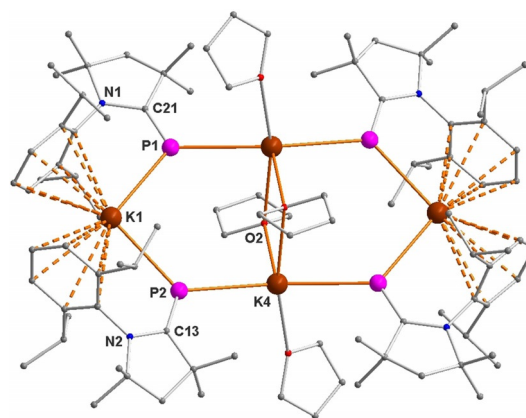


Figure 4. Molecular structure of complex **4-2THF**. Hydrogen atoms and two solvated THF molecules were omitted for clarity. Important bond lengths [Å] and bond angles [°]: C21–P1 1.702(3), C13–P2 1.703(3), C21–N1 1.402(3), C13–N2 1.401(3), P1–K1 3.2893(10), P2–K1 3.2314(9), P1–K4 3.2761(10), P2–K4 3.3532(10), K4–O1 2.885(3), K4–O2 2.763(3) and 2.954(3), N1–C21–P1 126.53(19), N2–C13–P2 127.93(19), C21–P1–K4 120.86(9), C21–P1–K1 115.19(9), K1–P1–K4 123.87(3), P2–K1–P1 97.49(2).

(2,6-diisopropylphenyl) in η^6 fashion. The position of $\text{Na3}/\text{Na3}'$ is slightly disordered leading to a boat like Na_3P_3 core. The chair like Na_3P_3 core was not observed in the solid state. The average C–P bond distance in the cyclic-trimer is found to be 1.701 Å, which falls in the range of previously reported carbene stabilized phosphinidenes.^[4a,7c,8,10,15] The P-atom of $\text{Cy-cAAC}=\text{P}^-$ possesses a near trigonal planar geometry with the sum of the bond angle close to 360° . The average Na–P distances in the cyclic-trimer are lying in the range of 2.757(2)–2.882(5) Å (Table S1) which are shorter than those (2.9246(8)–3.0178(8) Å) of the dimeric $(\text{Dipp})_2\text{PNa}(\text{THF})_2$ complex.^[6c] The average Na–

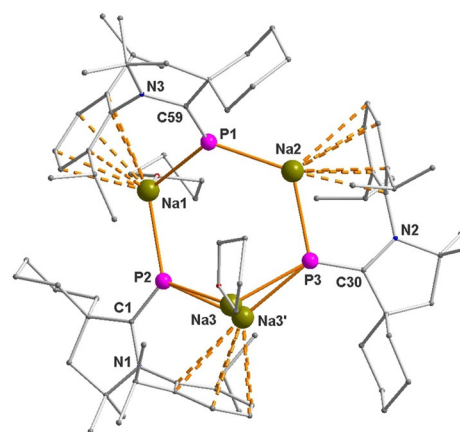


Figure 5. Molecular structure of complex **5-2THF**. Hydrogen atoms and two solvated THF molecule were omitted for clarity. Both coordinated THF molecules have half occupancies. The position of $\text{Na3}/\text{Na3}'$ is slightly disordered. Selected experimental [calculated at M06-2X/def2SVP] bond lengths [Å] and bond angles [°]: C1–P2 1.703(4) [1.708], C1–N1 1.405(6) [1.392], C59–P1 1.698(5) [1.711], C59–N3 1.402(6) [1.392], P1–Na1 2.850(2) [2.821], P1–Na2 2.757(2) [2.747], P2–Na1 2.831(2) [2.826], P3–Na2 2.806(3) [2.784], P3–Na3 2.794(5) [2.777], N1–C1–P2 126.6(3) [127.3], P1–Na1–P2 111.42(7) [96.6], Na1–P2–Na3 114.9(2) [128.4], P3–Na3–P2 121.7(2) [125.6], P1–Na2–P3 120.30(8) [124.90], Na2–P1–Na1 120.91(7) [130.00], Na3–P3–Na2 107.9(2) [100.40].

P-Na/P-Na-P bond angles in **5** are found in the range of $107.9(2)$ – $123.14(14)$ °/ $111.42(7)$ – $121.7(2)$ °.

To understand the bonding and electron density distribution of dimer **2** and trimer **5**, geometry optimization and vibrational frequency analysis were carried out at M06-2X/def2SVP level of theory (see Supporting Information for computational details). Natural Population Analysis (NPA) of **5** indicates NPA charge of -0.56 to $-0.59e$ on P atom, $+0.82$ to $+0.84e$ on Na atom and $-0.09e$ on C_{CAAC} (Table S16). The lowered NPA charge on P atom can be explained by the charge delocalization, additional P–Na interaction and strong π -acceptance by C_{CAAC} atom.

NBO analysis of **5** indicates a Wiberg Bond Index (WBI) of 1.68 – 1.69 (Table S17) for the C_{CAAC} –P bond, thereby suggesting a partial double bond. WBI (1.68 – 1.69) of C_{CAAC} –P bond of the trimer (**5**) has slightly lower value (1.68 – 1.69) than that of the dimers (**2**, see SI) (1.77 – 1.79). The σ type bond between C_{CAAC} and P has an occupancy of $1.97e$ with electron density heavily polarised towards C_{CAAC} (around 66%) and only 34% polarised towards the P atom indicating a dative bond. The second bond (π type) is formed by P atom donating back its electron density to the vacant p_z -orbital of C_{CAAC} with an occupancy of $1.95e$. However, in this case the electron density is slightly polarised towards the P atom (54% on P and 45% on C_{CAAC}). QTAIM analysis shows that the C_{CAAC} –P bond is a donor–acceptor type bond, whereas the P–Na bond is ionic in nature (Table S18). NBO analysis shows that HOMO, HOMO-1 and HOMO-2 are majorly the two lone pairs of electrons each localized on P atom (Figure 6). HOMO-3, HOMO-4 and HOMO-5 represent the π -backdonation from P to C_{CAAC} which have partial occupancy ($1.91e$ – $1.83e$) indicating the charge delocalization. The lone pair of P-atom with occupancy of $1.91e$ has 75% of s -character and 25% of p -character, while, the other lone pair with occupancy of $1.83e$ has 97% of p -character.

In conclusion, we have reported the syntheses and solid state characterization of cAAC-supported oligomeric potassium- and sodium-phosphinidenides (**2a/3–5**) by the reduction of cAAC-chlorophosphinidenes (**1**) using K/KC₈/Na-naphthalene as reducing agents. The quasi-reversible one electron reduction of **1a** observed from the cyclic voltammogram indicated the possible formation of the reactive radical intermediate (cAAC=P) which can dimerize to form (cAAC)₂P₂. The later upon further reduction (indicated by CV) can convert to monomeric species cAAC=P–K/Na leading to the formation of different oligomers (dimer **2a**, trimer **5**, tetramer **4** and hexamer **3**) in the solid state. Oligomerization of this class of complexes in the solid state has been found to be largely dependent on the charge accumulation on P-atom as evident by the significantly different calculated NPA charges on P-atoms of (cAAC)P–M (M=Li, K, Na), steric bulk of cAACs and ionic radius of the alkali metal ions.

Acknowledgements

S.R. (ECR/2016/000733) and K.C.M. (ECR/2016/000890) gratefully acknowledge SERB, New Delhi for their individual ECR grants. A.K. thanks KYPY for financial support; P.G.R., E.N. thank

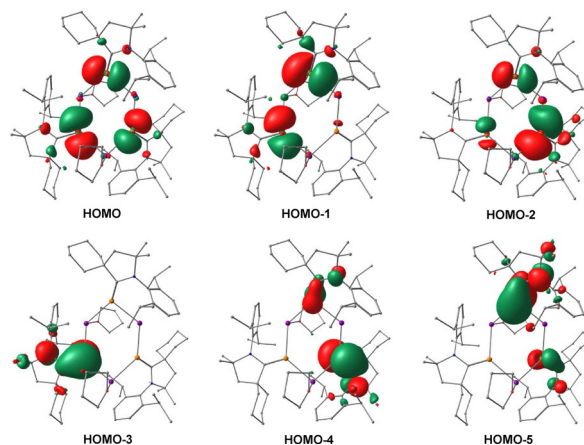


Figure 6. Representative molecular orbitals of complex **5** at M06-2X/def2TZVPP level of theory. Hydrogen atoms are omitted for clarity.

IISER Tirupati for Postdoctoral Fellowship and SRF, respectively. S.A., S.M.N.V.T.G. thank CSIR for SRF and M.F. for J.R.F. We thank Dr. P.K.S. Antharjanam for resolving the X-ray structural disorder.

Conflict of interest

The authors declare no conflict of interest.

Keywords: cyclic alkyl(amino) carbene • cyclic voltammetry • DFT calculations • oligomerization • phosphinidenide

- [1] H. Aktas, J. C. Slootweg, K. Lammertsma, *Angew. Chem. Int. Ed.* **2010**, *49*, 2102; *Angew. Chem.* **2010**, *122*, 2148.
- [2] a) A. Ecker, U. Schmidt, *Chem. Ber.* **1973**, *106*, 1453; b) G. Huttner, H.-D. Muller, A. Frank, H. Lorenz, *Angew. Chem. Int. Ed. Engl.* **1975**, *14*, 705; *Angew. Chem.* **1975**, *87*, 714; c) L. Liu, D. A. Ruiz, F. Dahcheh, G. Bertrand, *Chem. Commun.* **2015**, *51*, 12732.
- [3] a) Y. Wang, Y. Xie, M. Y. Abraham, R. J. Gilliard, Jr., P. Wei, H. F. Schaefer III, P. v. R. Schleyer, G. H. Robinson, *Organometallics* **2010**, *29*, 4778; b) A. Doddi, D. Bockfeld, T. Bannenberg, P. G. Jones, M. Tamm, *Angew. Chem. Int. Ed.* **2014**, *53*, 13568; *Angew. Chem.* **2014**, *126*, 13786; c) M. Cicač-Hudi, J. Bender, S. H. Schlindwein, M. Bispinghoff, M. Nieger, H. Grützmacher, D. Gudat, *Eur. J. Inorg. Chem.* **2016**, 649.
- [4] a) O. Back, M. Henry-Ellinger, C. D. Martin, D. Martin, G. Bertrand, *Angew. Chem. Int. Ed.* **2013**, *52*, 2939; *Angew. Chem.* **2013**, *125*, 3011; b) S. Roy, K. C. Mondal, S. Kundu, B. Li, C. J. Schermann, S. Dutta, D. Koley, R. Herbst-Irmer, D. Stalke, H. W. Roesky, *Chem. Eur. J.* **2017**, *23*, 12153.
- [5] K. Hansen, T. Szilvási, B. Blom, S. Inoue, J. Epping, M. Driess, *J. Am. Chem. Soc.* **2013**, *135*, 11795.
- [6] a) E. Hey-Hawkins, E. Sattler, *J. Chem. Soc. Chem. Commun.* **1992**, 775; b) E. Hey, P. B. Hitchcock, M. F. Lappert, A. K. Rai, *J. Organomet. Chem.* **1987**, *325*, 1; c) K. Izod, P. Evans, P. G. Waddell, *Dalton Trans.* **2017**, *46*, 13824; d) I. Jevtovikj, R. Herrero, S. Gómez-Ruiz, P. Lönnecke, E. Hey-Hawkins, *Inorg. Chem.* **2013**, *52*, 4488; e) K. Izod, J. Stewart, E. R. Clark, W. Clegg, R. W. Harrington, *Inorg. Chem.* **2010**, *49*, 4698; f) R. A. Bartlett, M. M. Olmstead, P. P. Power, *Inorg. Chem.* **1986**, *25*, 1243; g) M. Driess, G. Huttner, N. Knopf, H. Pritzkow, L. Zsolnai, *Angew. Chem. Int. Ed. Engl.* **1995**, *34*, 316; *Angew. Chem.* **1995**, *107*, 354; h) G. W. Rabe, G. P. A. Yap, A. L. Rheingold, *Inorg. Chem.* **1997**, *36*, 1990; i) G. W. Rabe, S. Kheradmandan, G. P. A. Yap, *Inorg. Chem.* **1998**, *37*, 6541.
- [7] a) G. Fritz, W. Holderich, *Z. Anorg. Allg. Chem.* **1976**, *422*, 104; b) M. Bispinghoff, A. M. Tondreau, H. Grützmacher, C. A. Faradji, P. G. Pringle, *Dalton Trans.* **2016**, *45*, 5999; c) O. Lemp, M. Balmer, K. Reiter, F. Weigend, C. von Hänisch, *Chem. Commun.* **2017**, *53*, 7620.

- [8] S. Kundu, S. Sinhababu, A. V. Luebben, T. Mondal, D. Koley, B. Dittrich, H. W. Roesky, *J. Am. Chem. Soc.* **2018**, *140*, 151.
- [9] For in situ generated NHC=P-K, see a) M. Balmer, Y. J. Franzke, F. Weigend, C. v. Hänisch, *Chem. Eur. J.* **2020**, *26*, 192; b) A. M. Tondreau, Z. Benkő, J. R. Harmer, H. Grützmacher, *Chem. Sci.* **2014**, *5*, 1545.
- [10] S. Kundu, S. Sinhababu, M. M. Siddiqui, A. V. Luebben, B. Dittrich, T. Yang, G. Frenking, H. W. Roesky, *J. Am. Chem. Soc.* **2018**, *140*, 9409.
- [11] M. Balmer, F. Weigend, C. v. Hänisch, *Chem. Eur. J.* **2019**, *25*, 4914.
- [12] O. Back, B. Donnadieu, P. Parameswaran, G. Frenking, G. Bertrand, *Nat. Chem.* **2010**, *2*, 369.
- [13] K. C. Mondal, P. P. Samuel, H. W. Roesky, R. R. Aysin, L. A. Leites, S. Neudeck, J. Lübber, B. Dittrich, N. Holzmann, M. Hermann, G. Frenking, *J. Am. Chem. Soc.* **2014**, *136*, 8919.
- [14] J. L. Rutherford, D. B. Collum, *J. Am. Chem. Soc.* **2001**, *123*, 199.
- [15] a) L. Weber, U. Lassahn, H.-G. Stämmler, B. Neumann, *Eur. J. Inorg. Chem.* **2005**, 4590; b) S. Kundu, B. Li, J. Kretsch, R. Herbst-Irmer, D. M. Andrada, G. Frenking, D. Stalke, H. W. Roesky, *Angew. Chem. Int. Ed.* **2017**, *56*, 4219; *Angew. Chem.* **2017**, *129*, 4283.

Manuscript received: July 28, 2020

Revised manuscript received: August 12, 2020

Accepted manuscript online: August 18, 2020

Version of record online: November 27, 2020